Torque and Flux Ripple Minimization of Induction Motor Using Space Vector Modulator

Adel Rafa [1]
[1]Faculty of Engineering Tobruk
Omar Al-Mukhtar University Libya
Adel_rafa@yahoo.com

Abdelnasser Nafeh[2]
[2] Faculty of Engineering Benha
Benha University Egypt
abdelnassern@yahoo.com

***Abstract*— direct torque control (DTC) of induction motor is known to have a simple control structure with comparable performance to that of the field-oriented control technique (FOC). But there are two major problems that are usually associated with DTC drives are: 1) switching frequency that varies with operating conditions and 2) high torque and flux ripples. To solve these problems, and at the same time retain the simple control structure of DTC, a constant switching frequency torque controller is proposed to replace the conventional hysteresis-based controller. In this paper, the simulation of proposed controller followed by experimental results is presented. The proposed controller is shown to be capable of reducing the torque and flux ripples and maintaining a constant switching frequency which gives a better dynamic performance than the conventional methods.**

Index Terms—**Direct torque and flux control, constant switching frequency, induction motor, space vector modulator.**

I. INTRODUCTION

IN RECENT years, marked improvement based on the development of micro processors and power electronics has been achieved in motor drives. However, motors driven by solid state inverters have undergone serious voltage stress of rapid switch-on and switch–off voltage of semiconductor devices. The induction motors are robust, easily maintained and reliable. Moreover the cost is lower, as well as the inertia and the weight compared to other machines. The variable speed operation of the induction machine is achieved by modern inverters. Fast switching frequency inverters are now available at relatively low price. The modern induction machines are now replacing DC motors in industry applications, even in the applications where a fast speed and torque response in four quadrants is required. One of the reliable techniques to effectively control the speed of induction motor is the Direct Torque Control (DTC) technique proposed by Takahashi [1]. This technique can be considered as an alternative to the Field Oriented Control (FOC) strategy [2]. In recent years the use of AC drives with DTC technique have gradually increased due to its advantages over the FOC techniques: good dynamic performance, precise and quick control of stator flux and electromagnetic torque, robust against machine parameters variations, no current control loop, and the simplicity of the algorithm [3,4]. A classical DTC drive system, which is based on a fixed hysteresis bands for both torque and flux controllers, suffers from a varying switching frequency, which is a function of the motor speed, stator/rotor fluxes, and stator voltage; it is also not constant in steady state. Variable switching frequency is undesirable. At low speed, an appreciable level of acoustic noise is present, which is mainly due to the low inverter switching frequency. The high frequency is limited by the switching characteristics of the power devices. Therefore, there will be large torque ripples and distorted waveforms in currents and fluxes. Several solutions have been proposed to keep constant switching frequency, like in [2-8,24,25,30,32,33,34-42]. In order to improve the dynamic performance of the classical DTC, a new modified DTC with a space vector modulator (SVM), and fuzzy logic controller (FLC) is proposed. The use of SVM is to ensure a constant switching frequency and the use of FLC is to obtain a decoupled control between flux and torque. The present paper deals with the development of a Fuzzy Logic Direct Torque Controller (FLDTC) that is expected to improve the dynamic performance compared to the classical DTC system. The study will cover the possible ways to overcome the disadvantages of the classical DTC method such as, starting problems, distorted current waveforms, variable switching frequency, and existence of high torque pulsation and flux ripple. This new DTFC system is firstly designed and proved by means of simulations. Later in the paper, experimental implementation is discussed and the results are presented.

II. LITERATURE REVIEW

The development of this novel induction motor controller can be separated into the following contributed steps: First, Study the classical DTC disadvantages and suggestion of new scheme to overcome them. Second, investigate of a complete dynamic model of the drive systems, relevant controllers, and its dynamic performance using MATLAB-SIMULINK and FUZZY LOGIC toolboxes. Third, implementation of an actual drive system based on micro controller and suggested DTFC to validate its performance practically. The conventional DTC drive system based on fixed hysteresis bands for both torque and flux controllers, suffers from varying switching frequency, which is undesirable and has bad effects on the dynamic performance of the drive systems. Therefore, there will be a large torque ripples and distorted waveforms in currents and fluxes. Several solutions have been proposed to keep constant switching frequency, like in [2-8,18,24,25,30,32,33,35]. The hysteresis regulators are difficult to be implemented in a discrete form even high sampling

causes errors in torque regulation. The approach proposed in Ref. [17] replaces the hysteresis regulators with a discrete regulator. The control scheme based on back emf estimation. It gives better results, but the sampling time in structure still very high, computationally extensive, and parameter sensitive. The approach proposed in Refs. [23,27,28] gives good torque response and also, very low torque distortions in steady state, but the fuzzy structure of this regulators is very complicated due to many member ship functions, specially in flux angle fuzzification. This leads to a lot of fuzzy rules, which need a large memory and complicated software to be implemented. In ref. [4] the influences of the hysteresis bands on the DTC of an induction motor are analytically investigated, and the inverter switching frequency is predicted. A new approach of DTC based on space vector modulator SVM and two PI controllers is presented in Ref. [25] which provides a constant inverter switching frequency and significantly reduction of torque and speed ripple. Ref. [35] gives a constant inverter switching frequency, but it replaces the two PI controller of the above approach Ref. [25] with a two fuzzy controller and replaces the space vector modulation SVM block by a sinusoidal PWM one. The simulation results give a significant reduction of torque ripples. But, this approach did not indicates any experimental results, and needs a coordinate transformations from synchronous reference frame to stationary reference frame then to a, b, c frame which is complicated and time consuming in programming. There are two issues and problems in motion control. One is to make the resulting system of controller and plant robust against parameter variations and disturbances. The other is to make the system intelligent. This is possible with advanced control theory such as, Neural networks, Fuzzy logic, or Neuro-fuzzy. A new control strategy in discrete DTC based on adaptive Neuro-Fuzzy structure is presented in [2,5,8]. This approach gives fast and good dynamic performance. However, the system is based on two Digital Signal Processors DSPs, the first (main) processor implements the direct torque Neuro-Fuzzy control algorithm, whereas the second provides the vector modulation which make the drive system more complicated in interfacing and programming, and costly to be implemented. The analysis on the effects of both flux and torque hysteresis bands on DTC drive system performance is presented in Ref. [4]. It is to be noted that small flux hysteresis bands leads to sinusoidal current waveforms, while small torque hysteresis bands allow smoothed torque to be generated. On the other hand, small hysteresis bands determine high switching frequency thereby increasing the switching losses. To improve the stator fluxes estimation in steady state for DTC of induction motor, a phase and magnitude compensation for the voltage model based stator flux estimator with low pass filter is proposed in Ref. [31]. Significantly improved waveforms of flux and torque are obtained. The duty cycle value based on fuzzy logic is presented in Refs. [14,34]. By varying the duty cycle between its extreme values, it is possible to apply any voltage value to the motor. Therefore, the duty cycle has to be determined for each sampling period. However, this approach still uses the two-hysteresis controllers also the torque and flux waveforms still have distorted waveforms and a high computational effort are needed. A new hybrid fuzzy controller for DTC based induction motor drives is presented in Ref. [29]. The approach satisfies a significantly improvement in steady state torque and flux ripples. However, it still uses the look-up table of classical DTC also; the drive system has a variable switching frequency.

III. CONVENTIONAL DTC STRATEGY

The basic idea of DTC is when the torque is wanted to be increased, a voltage vector which increases the angle between the air gap flux linkage and the stator flux linkage is selected, and vice versa. A block diagram of a classical DTC system for an induction motor is shown in Fig.1. Two independent hysteresis (bang-bang) controllers control the motor torque and stator flux [2,8]. Therefore, the selection of hysteresis band control range will affect on the performance of the drive system [10]. The inverter switching patterns are generally directly as a function both of the torque error and of the flux error. By using only current and voltage measurements, it is possible to estimate the instantaneous stator flux and output torque. An induction motor model is then used to predict the voltage required to drive the flux and torque to the demanded values within a fixed time period. From Fig. 1. The inputs to the switching table block are the torque and flux error, and the stator flux angle information are used to select the suitable switching pattern. Many voltage selection strategies can be utilized as widely discussed in ref. [11,12].

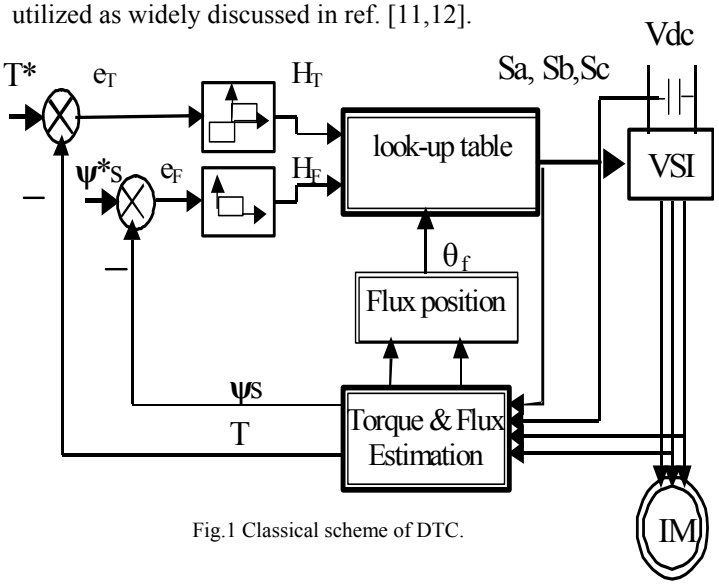

Fig.1 Classical scheme of DTC.

Each strategy affects the drive performance in terms of torque and current ripple, switching frequency, and torque response [10,11]. From Fig. 2. In order to increase the stator flux magnitude it is necessary to select the voltage vector that determines a high radial component along the direction of the stator flux vector ψs. On the other hand, if it is need to increase the torque, it is necessary to select the voltage vector that determines the highest tangential component along the direction of stator flux vector ψs [10,13]. The selection table proposed by Takahashi [1] is used as shown in Table 1.The sectors of the stator flux space vector are denoted from S1 to S6. The hysteresis controller for flux can take two different values, while the torque hysteresis controller can take three different values.

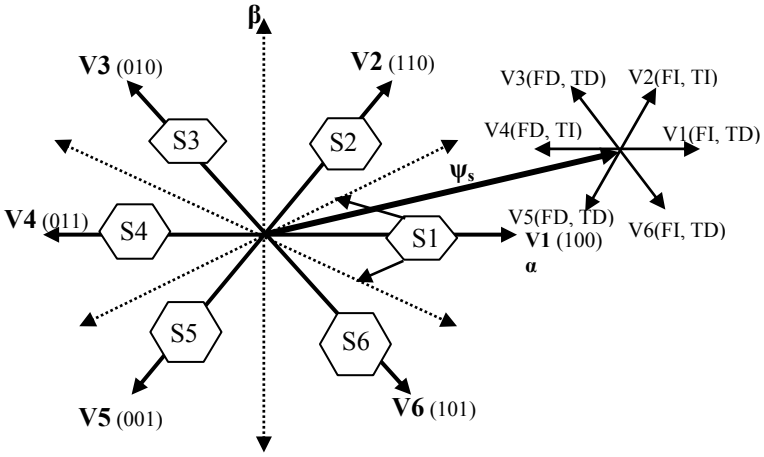

Fig. 2. Stator flux vector locus and different possible switching voltage vectors lies in sector 1.
F = Flux, T = Torque, D = Decrease, and I = Increase.

Table 1. Takahashi selection table for DTC.

H_F	H_T	S1	S2	S3	S4	S5	S6
1	1	V2	V3	V4	V5	V6	V1
1	0	V7	V0	V7	V0	V7	V0
1	-1	V6	V1	V2	V3	V4	V5
0	1	V3	V4	V5	V6	V1	V2
0	0	V0	V7	V0	V7	V0	V7
0	-1	V5	V6	V1	V2	V3	V4

The zero voltage vectors V0 and V7 are selected when the torque error is within the given hysteresis limits i.e. (in case of no change). To achieve our goals a mathematical modeling of the classical and proposed DTFC drive systems are obtained.

IV. MATHEMATICAL MODELING OF IM

The stationary reference frame labeled (α-β) dynamic model of the squirrel cage induction motor [18,22,26,36,37] with the reference frame fixed to the stator is given by:

$$\frac{d}{dt}\begin{bmatrix} i^s_{s\alpha} \\ i^s_{s\beta} \\ i^s_{r\alpha} \\ i^s_{r\beta} \end{bmatrix} = \frac{1}{L_\sigma^2}\left(\begin{bmatrix} L_r & 0 & -L_m & 0 \\ 0 & L_r & 0 & -L_m \\ -L_m & 0 & L_s & 0 \\ 0 & -L_m & 0 & L_s \end{bmatrix} \begin{bmatrix} v^s_{s\alpha} \\ v^s_{s\beta} \\ 0 \\ 0 \end{bmatrix} + \begin{bmatrix} -R_s L_r & \omega_r L_m^2 & R_r L_m & \omega_r L_r L_m \\ -\omega_r L_m^2 & -R_s L_r & -\omega_r L_r L_m & R_r L_m \\ R_s L_m & -\omega_r L_s L_m & -R_r L_s & -\omega_r L_r L_s \\ \omega_r L_s L_m & R_s L_m & \omega_r L_r L_s & -R_r L_s \end{bmatrix} \begin{bmatrix} i^s_{s\alpha} \\ i^s_{s\beta} \\ i^s_{r\alpha} \\ i^s_{r\beta} \end{bmatrix} \right) \quad (1)$$

Where

$$L_\sigma = \sqrt{L_s L_r - L_m^2}$$

$$\omega_r = \frac{P}{2}\omega_m$$

and the electromagnetic torque equation in the stationary reference frame:

$$T_e = \left(\frac{3}{2}\right)\left(\frac{Poles}{2}\right)\left(\psi_{s\alpha} i_{s\beta} - \psi_{s\beta} i_{s\alpha}\right) \quad (2)$$

Also, the dynamic equation of the motor can be written as:

$$T_e = J\frac{d\omega_m}{dt} + B\omega_m + T_L \quad (3)$$

For simulation and hardware minimization the stator output phase voltage of VSI can be computed from dc-link voltage and inverter switching states (Sa, Sb, Sc) instead of direct measuring with Hall effect voltage sensors as follows:

$$V_{as} = \frac{Vdc}{3}(2\,Sa - Sb - Sc) \quad (4)$$

$$V_{bs} = \frac{Vdc}{3}(2\,Sb - Sc - Sa) \quad (5)$$

$$V_{cs} = \frac{Vdc}{3}(2\,Sc - Sa - Sb) \quad (6)$$

Also, the two phase stationary reference frame voltages are:

$$V_{\alpha s} = V_{as} = \frac{Vdc}{3}(2\,Sa - Sb - Sc) \quad (7)$$

$$V_{\beta s} = \frac{V_{\alpha s} + 2V_{bs}}{\sqrt{3}} = \frac{Vdc}{\sqrt{3}}(Sb - Sc) \quad (8)$$

And for DTC modeling and implementation the stator flux vector ψ_s estimation can be calculated in stationary reference frame by integrating the motor back emf space vector, measured stator currents, and stator resistance as follows:

$$\psi_{\alpha s} = \int (V_{\alpha s} - R_s i_{\alpha s})dt \quad (9)$$

$$\psi_{\beta s} = \int (V_{\beta s} - R_s i_{\beta s})dt \quad (10)$$

$$\psi_s = \psi_{\alpha s} + j\psi_{\beta s} \quad (11)$$

Where, the flux magnitude and its position can be determined from:

$$|\overline{\psi_s}| = \sqrt{\psi_{\alpha s}^2 + \psi_{\beta s}^2} \quad (12)$$

$$\theta_f = \tan^{-1}\left(\frac{\psi_{\beta s}}{\psi_{\alpha s}}\right) \quad (13)$$

By using the previous equations and the look up table the simulation of classical DTC is achieved. Unfortunately, a low speed and starting problems are exists with torque and flux ripples and variable switching frequency from hysteresis controllers which may damage and have a bad effect on the power switches of the inverters and the overall performance.

V. Analog and Digital Implementation of Hysteresis Controller

Since a DTC-based drive selects the inverter switching states using switching look-up table, neither current controllers nor pulse width modulation is required, thereby providing fast torque response. However, this switching table-based DTC approach has some disadvantages. This disadvantages are described as follows. For digital implementation, the system sampling frequency for the calculation of torque and flux should be very high to provide good tracking performance and limit the errors of the torque and the flux within the specified bands, respectively. Moreover, a large torque ripple is generated due to delay time caused by the necessary calculation time of DTC algorithms, the sluggish response of measured voltages and currents due to the Hall effect transudes delay, and the conversion time of the analog to digital converters A/Ds [11,14,15,22].

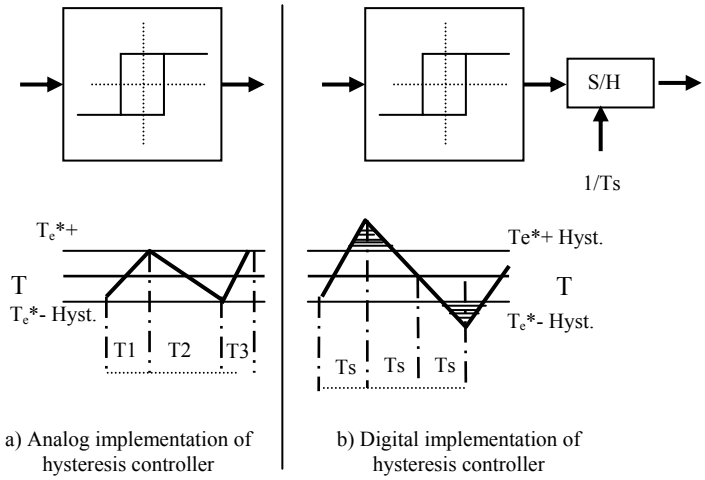

Fig. 3 Torque response for analog and digital implementation of Hysteresis controller.

Hence, if the DTC algorithm selects the optimum inverter switching state from the switching look-up table in one sampling period, the unavoidable delay between consecutive sampling would cause increased errors of both flux and torque. Therefore, the torque and flux couldn't be restricted within the specified Hysteresis bands. Many technical papers have concerned for improving of direct torque control performance like in [2,5,7,8,10,13,14,21]. Moreover, any digital implementation of the Hysteresis blocks introduces, an extra ripple, which depends on the sampling time (Ts) as illustrated in Fig. 3. An analog implementation would have constant ripple within its Hysteresis bands at the cost of no constant sampling time i.e. (the time between the samples is not constant) as shown in Fig 3 (a). On the contrary, in a digital implementation the time between each sample is constant but the ripple is variable and higher than the Hysteresis bands as shown in Fig 3 (b). Therefore, the digital Hysteresis block should also be represented with a sample and hold (S/H) working at the sampling frequency. In addition to the hardware delay there is also a software delay, which degraded the dynamic performance of the traditional DTC [11,14,15,21]. Alternatively, in this paper a new modified approach of DTC based on fuzzy logic and space vector modulator is presented. Fuzzy logic is introduced to make a decoupling control between the torque and flux and the SVM is incorporated with DTC for induction motor drives to provide a constant inverter switching frequency. To solve these problems, a space vector modulator SVM and Fuzzy Logic Controllers are used instead of look up table and Hysteresis controllers respectively.

VI. PROPOSED DTC STRATEGY

The proposed scheme is shown in Fig. 4 which shows the replacement of the two Hysteresis controllers of the classical DTC scheme with a fuzzy logic controller (FLC). Furthermore, it shows the replacement of the look-up table with a space vector modulator (SVM). The inputs to the FLC block are torque error e_T, flux error e_F, and the stator flux position information θ_f. The outputs of the fuzzy logic controller (FLC) are the desired space voltage vector V_s^* and its position angle θ_v. These two signals (V_s^*, θ_v) are used to be inputs to the space vector modulator (SVM) block, which in turn generates the suitable gating signals (Sa,Sb,Sc) to drive the inverter at a constant switching frequency.

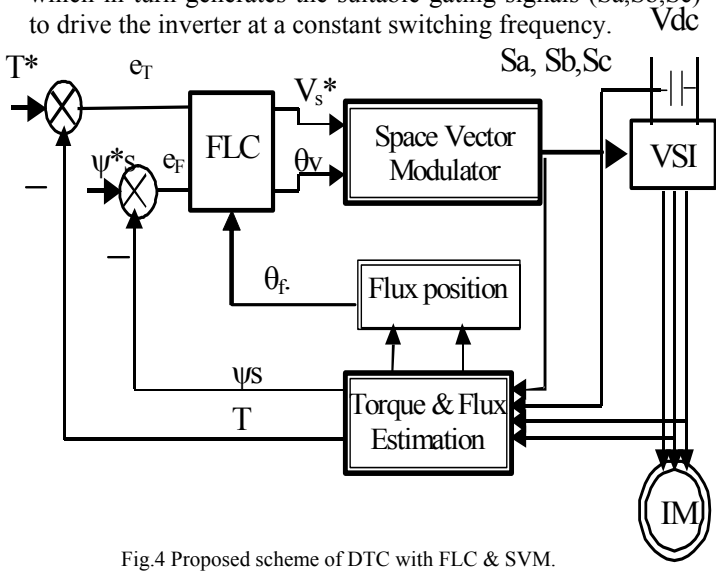

Fig.4 Proposed scheme of DTC with FLC & SVM.

The will-known disadvantages of the classical DTC such as [2-8]: Variable switching frequency, current and torque distortion due to sector changes start and low speed operation problems, and the high sampling frequency needed for digital implementation of Hysteresis controllers. All the above difficulties can be overcome with the use of the modified DTC scheme. Therefore, a constant inverter switching frequency, a torque ripple reduction, and a good dynamic performance can be obtained.

VII. Space Vector Modulator Calculations

Space vector modulation strategies, enables the switches of inverter between a selection of six active and two null states, to approximate a rotating vector representation of desired output voltages or currents [23-33]. It is known that any three-phase system can be transformed to an equivalent two-phase system, which has two orthogonal components. Its resultant vector is the rotating vector V_S, which describes the behavior of the three phases at any given time. This rotating vector is expressed as follows:

$$V_s = \frac{2}{3}[V_a + aV_b + a^2 V_c] \quad (14)$$

Where,

$$a = \left[-\frac{1}{2} + j\frac{\sqrt{3}}{2}\right] = e^{j\frac{2\pi}{3}} \quad (15)$$

$$a^2 = \left[-\frac{1}{2} - j\frac{\sqrt{3}}{2}\right] = e^{j\frac{4\pi}{3}} \quad (16)$$

Equation 14 is the general form for computing the rotating vector. This equation is valid for any three-phase system either balanced or unbalanced system. Detailed analysis is carried out in reference [23,32]. To compute the time periods for each space vector, equate the average time of the three switching state vectors - taken over the period to the reference vector, becomes:

$$V_s^* = V_j\frac{t_j}{T_S} + V_k\frac{t_k}{T_S} + V_0\frac{t_0}{T_S} + V_7\frac{t_7}{T_S} \quad (17)$$

$$V_s^* T_S = V_0 t_0 + V_j t_j + V_k t_k + V_7 t_7 \quad (18)$$

$$T_S = t_0 + t_j + t_k + t_7 \quad (19)$$

Where:
V^*_s is the desired space vector
T_s is the switching time (switching cyle)
t_0 , t_j, t_k, and t_7: are the time intervals
$V_0$and V_7 are two zero vectors
V_j and V_k are the vectors adjacent to V^*_s.
To determine these time intervals, the reference space vector is resolved into two components V_j along direction V_2 and V_k along direction V_3 as shown in Fig. 5 This gives the following equations:

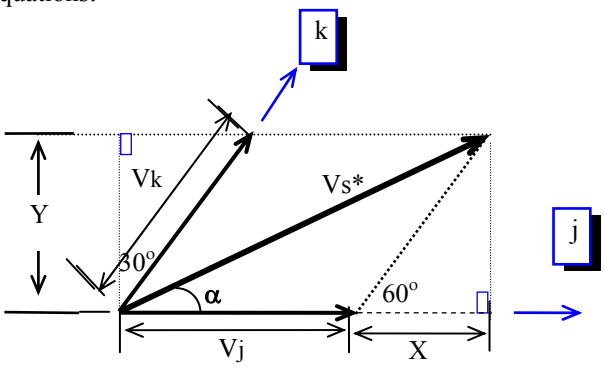

Fig. 5 Space vector approximation.

$$X = V_k \cos(60) = V_k/2 \quad (20)$$

$$Y = V_s^* \sin(\alpha). \quad (21)$$

$$V_k = \frac{Y}{\cos 30} = Y\left(\frac{2}{\sqrt{3}}\right) = \left(\frac{2}{\sqrt{3}}\right)V_s^* \sin(\alpha) \quad (22)$$

$$V_j = V_s^* \cos(\alpha) - X. \quad (23)$$

Substitutes from Eqns. 20 & 22 in Eqn. 23 yields:

$$V_j = V_s^*\left[\cos\alpha - \frac{1}{\sqrt{3}}\sin\alpha\right] \quad (24)$$

$$V_k = V_s^*\left[\frac{2}{\sqrt{3}}\sin\alpha\right] \quad (25)$$

The times t_j , t_k, and T_S are proportional to components V_j , V_k, and 2/3 V_{dc} respectively. Then the time intervals can be found as follows:

$$t_j = 3/2\ V_j * T_s/ V_{dc} \quad (26)$$

and

$$t_k = 3/2\ V_k * T_s/ V_{dc} \quad (27)$$

Substituting from Eqns. 24 and 25 in Eqns. 26 and 27. Then the time intervals can be found as follows:

$$t_j = \frac{3}{2}\frac{V_s^*}{V_{dc}}T_S\left[\cos\alpha - \frac{1}{\sqrt{3}}\sin\alpha\right] \quad (28)$$

and

$$t_k = \frac{3}{2}\frac{V_s^*}{V_{dc}}T_S\left[\frac{2}{\sqrt{3}}\sin\alpha\right] \quad (29)$$

$$t_0 + t_7 = T_S - (t_j + t_k) \quad (30)$$

The null voltage vector times are simply shown as their sum. The individual values of t_0 and t_7 are arbitrarily chosen [23,32]. The strategy used is to divide the total null time equally between both t_0 and t_7. The maximum amplitude of fundamental component phase voltage using previously defined space vector modulator is:

$$V_{1\max} = \frac{1}{\sqrt{3}}V_{dc} \quad \text{For circular trajectory} \quad (31)$$

By using SVM equations, the estimation of stator flux can be improved and a good dynamic performance of the proposed DTFC with good waveforms can be obtained.

VIII. SYSTEM SIMULATION

The objective of this part is to illustrate the simulation of the conventional and proposed systems to consolidate the theoretical analysis of the paper. The simulation work conducted in this paper is based on, Matlab / Simulink

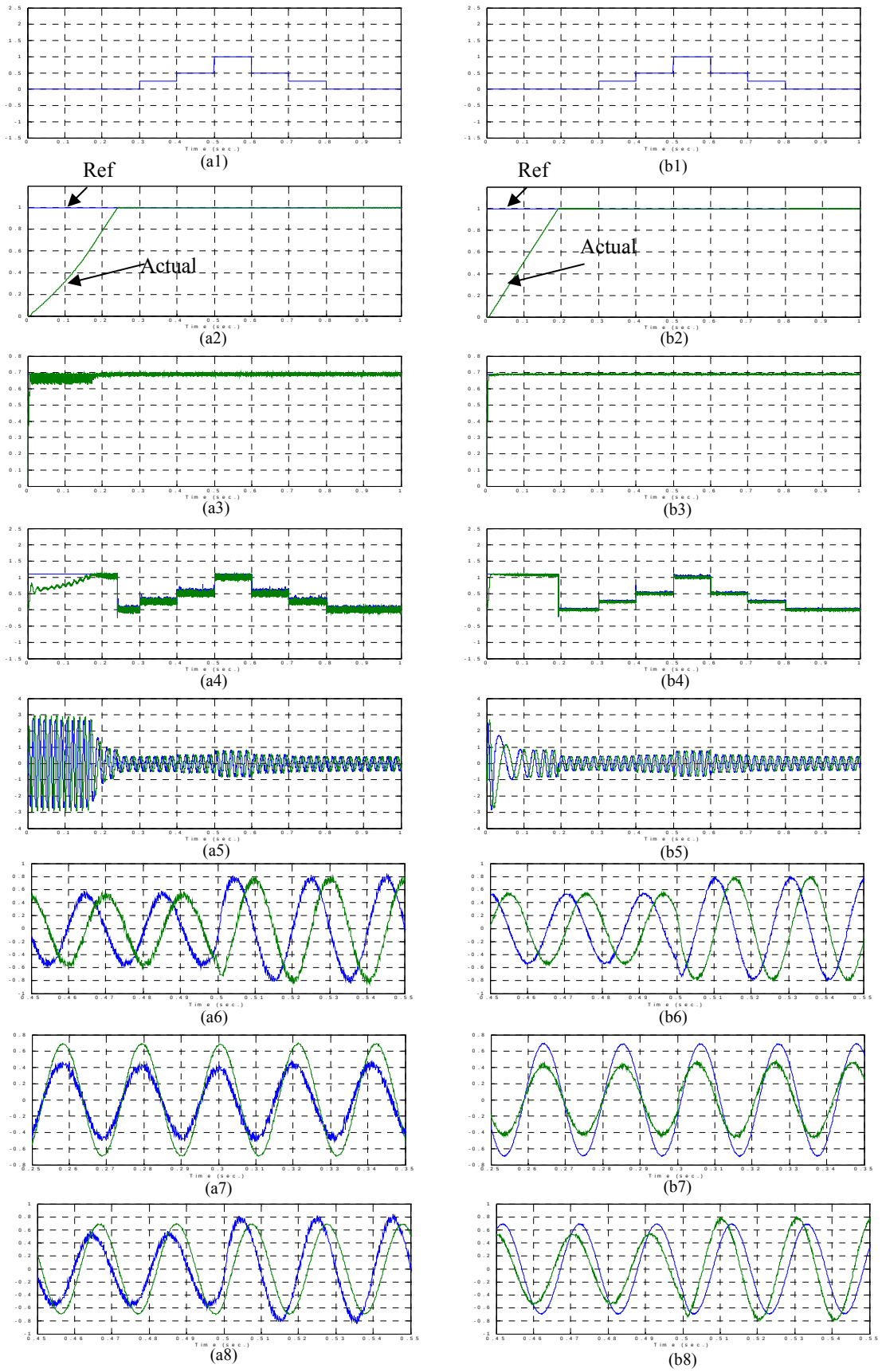

(a) Classical DTC results

(b) Proposed DTC results

Fig. 6 Dynamic performances of DTC schemes at different conditions.

programming and Fuzzy Logic toolbox. Other features of machine response can be extracted from the simulation of the drive motor model during sudden load changes. A series of simulated results have been carried out to verify the validity of the control scheme of the drive systems for direct torque control techniques. The results were obtained at different operating points including the step change in load. Some of these results are indicated in Figs. 6 (a) and (b) for both classical and proposed DTC schemes respectively. The simulated load torque of the tested systems is shown in Figs. 6 (a1) and (b1) as indicated from these figures that the machine is not loaded until the instant at (t = 0.3) sec. At (t = 0.3) sec., the drive system was subjected to sudden load change from (0 % to 25 %) of the rated torque. At (t = 0.4) sec., the drive system was subjected to sudden load change from (25 % to 50 %) of the rated torque. At (t = 0.5) sec., the drive system was subjected to sudden load change from (50 % to 100 %) of the rated torque. At (t = 0.6) sec., the drive system was subjected to sudden load change from (100 % to 50 %) of the rated torque. At (t = 0.7) sec., the drive system was subjected to sudden load change from (50 % to 25 %) of the rated torque. Finally, at (t = 0.8) sec., the drive system was subjected to sudden load change from (25 % to 0 %) of the rated torque. The corresponding dynamic responses for these sudden changes of loads are indicated in Figs. 6 (a) and (b) for both drive systems. The estimated flux is constant all over the operating period while; the currents and torque are increased or decreased to match the desired load. The speed in proposed system is reached its steady state value faster than the classical one. Moreover, the flux and torque ripple is smaller than that of classical one. Figures 6 (a6) and (b6) show the two-phase stationary reference frame current components during sudden change of load. They are perpendicular to each other and the current amplitudes are increased due to load torque increased and vice versa. The direct components of current and flux are shown in Figs. 6 (a7) and (b7). At no load the speed of the machine is relatively high and the resistance value can be neglected with respect to the inductive reactance value so, the direct component of currents are nearly in phase with that of the direct component of flux. At loading there will be a small displacement angle between the current and flux component and the current is increased as indicated in Figs. 6 (a8) and (b8). The simulation results of the conventional and proposed drive systems are based mainly on a 2.2kW three-phase induction motor and the previously mentioned equations. Figure 6 represents the simulation results of the complete inverter drive systems. These arrangements are obtained from the two drive systems and distributed by the same manner as shown in Fig. 6. The dynamic behavior of the two DTC schemes with torque and flux hysteresis bands equals to 0.1 % which corresponding to an average switching frequency of 28.11 kHz for classical DTC and a constant switching frequency of 5 kHz for the proposed DTC is shown in Fig. 6. It can be noticed from Fig. 6 that, when the torque and flux hysteresis band are decrease the response of the classical DTC drive system becomes better but the average switching frequency in increased and becomes unpredictable. The unpredictable switching frequency may damage the power devices of the inverter and has a bad effect on the overall performance therefore; the switching losses are increased [2-8,11,13,20]. But by using our proposed DTC drive system a controllable and lower switching frequency with a very good dynamic performance are achieved.

IX. SYSTEM IMPLEMENTATION

The objective of this part is to illustrate the experimental set up of the implemented system to consolidate the theoretical analysis of the paper. The experimental work conducted in this paper is based on, the micro-controller variable speed cage drive system running under different conditions. Test results are compared with simulation and the necessary discussions are mentioned.

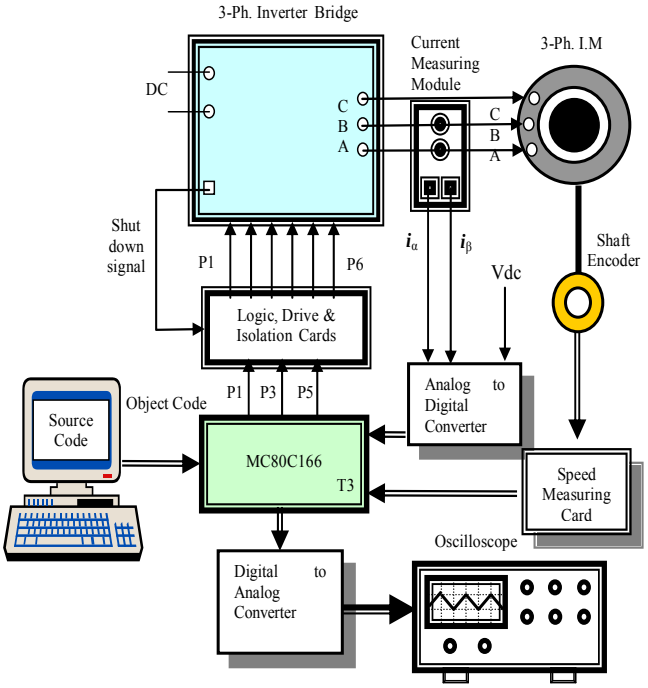

Fig. 7. Connection diagram of the implemented DTC system.

The experimental results of this proposed drive system are based mainly on a 2.2kW three-phase induction motor and displayed facilities using four-channel digital storage oscilloscope 'Tektronix-TDS2014'. The results are recorded by snap shots of different examined cases and then analyzed when required. Figure 7 represents the schematic connection between the different modules in the complete inverter drive system. The figure indicates that the main elements of the experimental system arranged for this study are: the PC with the necessary software and the interfacing developed specially for this investigation, the micro-controller, family MC80C166, the data acquisition logic card acting as an interface between the micro-controller and the 3-phase inverter circuits, Hall-effect current sensors essentially to measure the actual current under any operating condition and then used to compute the (α-β) current components in the stationary (α-β) reference frame, Hall-effect voltage sensor essentially to measure the actual DC-link voltage under any operating condition and then used to compute the (α-β) voltage components in the stationary (α-β) reference frame

with the aid of the switching states (Sa, Sb, and Sc), and the examined 3-phase induction motor. Fig. 8 shows some partial results of the proposed DTC using SVM technique and fuzzy logic controller. The experimental results are performed at a constant switching frequency of 5 kHz. Then a torque and flux ripples minimization can be obtained by using the suggested scheme.

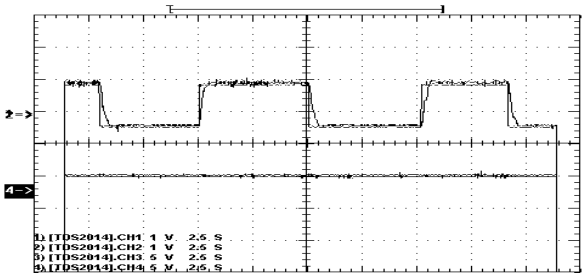

Fig. 8.a Reference & actual speed and reference & actual flux. (CH1 & 2: 0.4 p.u. /div, CH3 & 4: 1 p.u. /div & Time: 2.5 s/div)

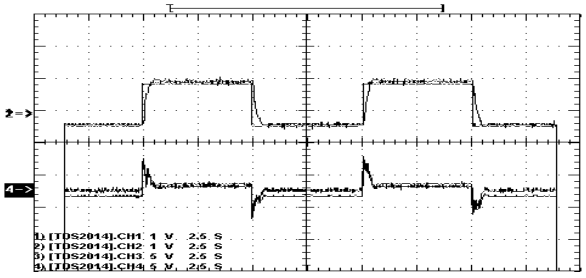

Fig. 8.b Reference & actual speed and reference & actual torque. (CH1 & 2: 0.4 p.u. /div, CH3 & 4: 1 p.u. /div & Time: 2.5 s/div)

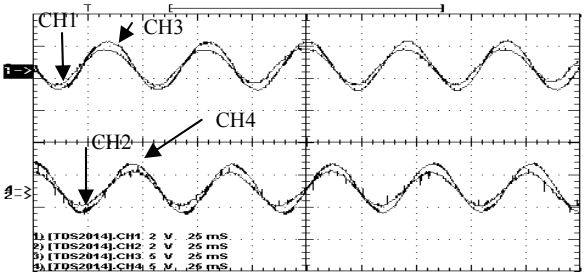

Fig. 8.c Performance of system fluxes and currents at no load.(CH1 (I alpha): 0.8 p.u. /div, CH3 (flux alpha): 1 p.u. /div, CH2 (I beta): 0.8 p.u. /div, CH4 (flux beta): 1 p.u. /div, & Time: 25 ms /div)

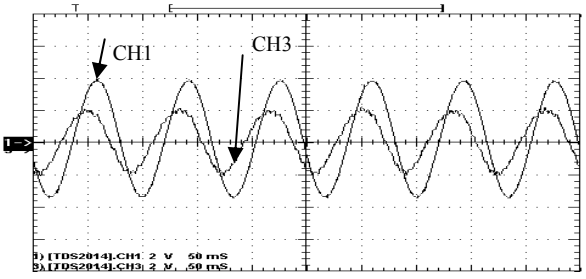

Fig. 8.d Performance of flux alpha and I alpha during loading. (CH1 (flux alpha): 0.4 p.u. /div, CH3 (I alpha): 0.8 p.u. /div, & Time: 50 ms /div)

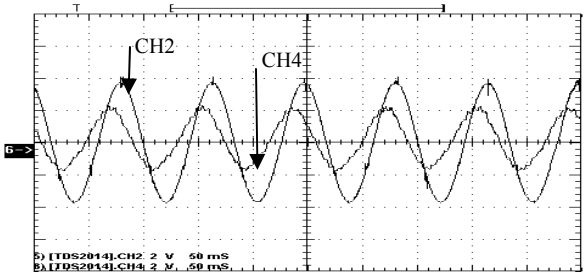

Fig. 8.e performance of flux beta and I beta during loading.(CH2 (flux beta): 0.4 p.u. /div, CH4 (I beta): 0.8 p.u. /div, & Time: 50 ms /div)

X. CONCLUTION

This paper presents a novel control method for DTFC of squirrel cage induction motor fed by a Space Vector Pulse Width Modulation voltage source inverter. The control strategy is based on fuzzy logic control and space vector modulator. The proposed controller has been tested in order to verify its behavior. The simulation and experimental results was proved that the controller ensured good response in operation near zero rotor speed and also good dynamic performance. The suggested system has a low cost price achieved by using MC80C166. From the simulations and experimental results of the proposed scheme it can be noted that a very good dynamic and steady state performance are achieved under different conditions with torque and flux ripples minimizations with a lower and constant switching frequency.

XI. APPENDIX

Table 2. Induction motor parameters and closed loop controller parameters

Type :	3-phase delta connected squirrel cage induction motor.
Rated power:	2.2 kW
Rated stator line voltage:	380V
Line current :	5.3 A
Frequency :	50 Hz
Number of poles :	4
Rated speed :	1420 rpm
Stator resistance Rs :	11 ohm/phase
Rotor resistance referred to stator R_r :	3.2 ohm/phase
Stator inductance L_s:	0.3713 H
Rotor inductance referred to stator L_r:	0.3713 H
Magnetizing inductance L_m:	0.3438 H
Mass moment of inertia of the motor J:	0.02 kg.m^2
Parameters of close loop controllers	
Proportional Controller	10
Integral Controller	0.06

XII. REFERENCES

[1] I. Takahachi and T. Noguchi, "A new quick response and high efficiency control strategy of an induction machine", IEEE Trans. on Ind. Applications, Vol.IA-22, pp. 820-827, Sept./Oct. 1986.

[2] Pawel Z. Grabowski, M. P. Kazmierkowski, B. K. Bose, and Frede Blaabjerg, " A Simple Direct-Torque Neuro-Fuzzy Control of PWM-Inverter-Fed Induction Motor Drive", IEEE Trans. on Ind. Elec., Vol. 47, No. 4, pp. 863-870, Aug. 2000.

[3] D. Swierczynski, M. P. Kazmierkowski, and F. Blaabjerg, " DSP Based Direct Torque Control of Permanent Magnet Synchronous Motor (PMSM) Using Space Vector Modulation (DTC-SVM)", Proc. of IEEE' 2002, pp. 723-727.

[4] D. Casadei, G. Grandi, G. Serra, and A. Tani, "Effects of Flux and Torque Hysteresis Band Amplitude in Direct Torque control of Induction Machines", Proc. of IEEE IECON'94, Bolongna, Italy, Sept. 1994, pp. 299-304.

[5] Pawel Z. Grabowski, and Frede Blaabjerg, "Direct Torque Neuro-Fuzzy Control of Inducion Motor Drive DSP Implementation", Proc. of IEEE IECON'98, Vol. 2, 1998, pp. 657-661.

[6] Jun-Koo Kang, and Seung-Ki Sul,"Analysis and Prediction of Inverter Switching Frequency in Direct Torque Control of Induction Machine Based on Hysteresis Band and Machine Parameters", IEEE Trans. on Ind. Elec., Vol. 48, No. 3, pp. 545-553, June 2001.

[7] Ahmed A. Mahfouz, Gamal M. Sarhan, and Abdel-Nasser A. Nafeh, "Direct Torque Control of Induction Motor Using Intelligent Controller", Proc. of IEEE MEPCON'03, Egypt, Vol. 1, Dec. 2003, pp. 345-349.

[8] Pawel Z. Grabowski, "Direct Torque Neuro-Fuzzy Control of Induction Motor Drive", Proc. of IEEE IECON'97, Japan, Vol. 2, 1997, pp. 557-562.

[9] A. Arias, et al, "Improving Direct Torque Control by means of Fuzzy Logic", Electronics Letters 4th Jan. 2001, Vol. 37, No. 1, pp. 69-71.

[10] M. P. Kazmierkowski and A. Kasprowicz, "Improved Direct Torque Control and Flux Vector Control of PWM Inverter-Fed Induction Motor Drives", IEEE Trans. Ind. Elec., vol. 45, pp. 344-350, Aug. 1995.

[11] C. Attaianese, et al, "Vectorial Torque Control (VTC): A Novel Approach to Torque and Flux Control of Induction Motor Drives", IEEE Trans. On Ind. Appl., Vol. 35, No. 6, Nov./Dec. 1999, pp. 1399-1405.

[12] T. G. Hableter, et al., " Direct Torque Control of Induction Machines Using Space Vector Modulation", IEEE Trans. Ind. App., vol. 28, pp. 1045-1053, Sept./ Oct. 1992.

[13] D. Casadei, et al, "Implementation of a Direct Torque Control Algorithm for Induction Motors Based on Discrete Space Vector Modulation", IEEE Tran. On Power Elec., Vol. 15, No. 4, July 2000, pp. 769-777.

[14] Kyo-Beum Lee, et al, "Torque Ripple Reduction in DTC of Induction Motor Driven by Three-Level Inverter with Low Switching Frequency", IEEE Trans. On Power Elec., Vol. 17, No. 2, March 2002, pp. 255-264.

[15] P. Marino, et al, "A Comparison of Direct Torque Control Methodologies for Induction Motor", Proc. of IEEE PPT'01, Proto-Portugal Power Tech. Conference, Sept. 2001.

[16] CG Mei, SK Panda, et al, "Direct Torque Control of Induction Motor-Variable Switching Sectors", IEEE PEDS'99, Hong Kong, July 1999, pp. 80-85.

[17] N.R.N. Idris and A.H.M. Yatim "Reduced Torque Ripple and Constant Torque Switching Frequency Strategy for Direct Torque Control of Induction Motor", Proc. of IEEE, APEC'00, 2000, pp. 154-161.

[18] S. A. Mir, D. S. Zinger, and M. E. Elbuluk, "Fuzzy Controller for Inverter Fed Induction Machines", IEEE Trans. On Industry Applications, Vol., 30, No. 1, Jan./Feb. 1994, pp.78-84.

[19] A. Tripathi, et el, " Space-Vector Based, Constant Switching Frequency, Direct Torque Control and Dead Beat Stator Flux Control of AC Machines", Proc. of IEEE IECON'01, 2001, pp. 1219-1224.

[20] Yen-Shin Lai, and Jian Ho Chen, "A New Approach to Direct Torque Control of Induction Motor Drives for Constant Inverter Switching Frequency and Torque Ripple Reduction", IEEE Trans. On Energy Conversion, Vol. 16, No. 3, Sept. 2001, pp. 220-227.

[21] Vector Perelmuter, "A Simplified Modeling of Induction Motor Drives with Direct Torque Control", Proc. of IEEE ISIE'99, Bled-Slovenia, 1999, pp. 486-491.

[22] S. A. Mir, M. E. Elbuluk, and D. S. Zinger, "Fuzzy Implementation of Direct Self Control of Induction Machines", IEEE Trans. On Industry Applications, Vol., 30, No. 3, May/June 1994, pp.729-735.

[23] S. A. Mir, M. E. Elbuluk, and D. S. Zinger, "PI and Fuzzy Estimators for Tuning the Stator Resistance in Direct Torque Control of Induction Machines", IEEE Trans. On Power Elec., Vol., 13, No. 2, March 1998, pp.279-287.

[24] Yen-Shin Lai, and Juo-Chiun Lin, "New Hybrid Fuzzy Controller for Direct Torque Control Induction Motor Drives", IEEE Trans. On Power Elec., Vol., 18, No. 5, Sept. 2003, pp.1211-1219.

[25] D. Casadei, et al, "Performance Analysis of a Speed Sensorless Induction Motor Drive Based on a Constant Switching Frequency DTC Scheme", IEEE Trans. On Industry Elec., Vol., 39, No. 2, March/April 2003, pp.476-484.

[26] N. R. N. Idris, A. M. Yatim, "An Improved Stator Flux Estimation in Steady State Operation for Direct Torque Control of Induction Machines", IEEE Trans. On Ind. App., Vol., 38, No. 1, Jan./Feb. 2002, pp.110-116.

[27] Jun-Koo Kang, and Seung-Ki Sul, "New Direct Torque Control of Induction Motor for Minimum Torque Ripple and Constant Switching Frequency", IEEE Trans. on Industry Applications, Vol. 35 No. 5 , Sep/Oct 1999 , pp. 1076 –1082.

[28] Purcell, A., and Acarnley, P.P., "Enhanced inverter switching for fast response direct torque control", IEEE Transactions on Power Electronics Vol16, No. 3, May 2001, pp. 382–389.

[29] E. E. El-kholy, et al, "Analysis and Implementation of A New Current Controller Based Space Vector Modulation for Induction Motor Drive", Proc. of IEEE MEPCON'03, Egypt, Vol. 1, Dec. 2003, pp. 143-149.

[30] M. Azab, "Improvement of Direct Torque Control Performance Using Fuzzy Logic Controllers" ", Proc. of IEEE MEPCON'03, Egypt, Vol. 1, Dec. 2003, pp. 185-190.

[31] P. Vas, Sensorless Vector and Direct Torque Control, Oxford, U.K. Oxford Univ. Press, 1998.

[32] A. M. Trzynadlowski, The Field Orientation Principle in Control of Induction Motors, Kluwer Academic Publishers, Norwell, Massachusetts, 1994.

[33] Giuseppe Buja, and Roberto Menis, "Steady-State Performance Degradation of a DTC IM Drive Under Parameter and Transduction Errors", IEEE Trans. On Industrial Electronics, Vol. 55, No. 4, April 2008.

[34] Kyo-Beum Lee, and Frede Blaabjerg, "An Improved DTC-SVM Method for Sensorless Matrix Converter Drives Using an Overmodulation Strategy and a Simple Nonlinearity Compensation", IEEE Trans. On Industrial Electronics, Vol. 54, No. 6, December 2007.

[35] Domenico Casadei, Giovanni Serra, Andrea Stefani, Angelo Tani, and Luca Zarri, "DTC Drives for Wide Speed Range Applications Using a Robust Flux-Weakening Algorithm", IEEE Trans. On Industrial Electronics, Vol. 54, NO. 5, October 2007.

[36] François Bonnet, Paul-Etienne Vidal, and Maria Pietrzak-David, "Dual Direct Torque Control of Doubly Fed Induction Machine", IEEE Trans. On Industrial Electronics, Vol. 54, No. 5, October 2007.

[37] Vivek Dutt, Rohtash Dhiman, "Comparative Study of Direct Torque Control of Induction Motor Using Intelligent Techniques", Canadian Journal on Electrical and Electronics Engineering Vol. 2, No. 11, November 2011.

[38] Kazmierkowski, M.; Karprowicz, A. Improved direct torque control and flux control of PWM inverter-fed induction motor drives, IEEE Trans. Ind. Electron., vol. 45, pp.344-350, 1995.

[39] T. G. Hableter, et al., " Direct Torque Control of Induction Machines Using Space Vector Modulation", IEEE Trans. Ind. App., vol. 28, pp. 1045-1053, Sept./ Oct. 1992.

[40] D. Casadei, et al, "Implementation of a Direct Torque Control Algorithm for Induction Motors Based on Discrete Space Vector Modulation", IEEE Tran. On Power Elec., Vol. 15, No. 4, July 2000, pp. 769-777.

[41] D. Casadei, et al, "Performance Analysis of a Speed Sensorless Induction Motor Drive Based on a Constant Switching Frequency DTC Scheme", IEEE Trans. On Industry Elec., Vol., 39, No. 2, March/April 2003, pp.476-484.

[42] G. Poddar, A. Joseph, and A. K. Unnikrishnan, "Sensorless Variable-Speed Controller for Exiting Fixed-Speed Wind Power Generator with Unity-Power-Factor Operation", IEEE Trans. On Industrial Elec., Vol., 50, No. 5, Oct. 2003, pp.1007-1115.